

ISSN 0891-3862

大气科学

CHINESE JOURNAL OF

ATMOSPHERIC
SCIENCES

(Scientia Atmospherica Sinica)

Volume 23 Number 4 1999

EDITED BY
Institute of Atmospheric Physics, Chinese Academy of Sciences

ALLERTON PRESS, INC. / NEW YORK

CHINESE JOURNAL OF ATMOSPHERIC SCIENCES

CONTENTS

VOLUME 23, NO. 4, 1999

- Atmospheric Circulation Evolutions Associated with Summer Monsoon Onset
in the South China Sea
Li Chongyin and Qu Xin..... 311
- Gearing between the Indo-Monsoon Circulation / Pacific-Walker Circulation
and ENSO. Part II: Simulation
Meng Wen and Wu Guoxiong 326
- Impact of Position and Horizontal-Scale of Strong Convection Area on the
Low-Frequency Oscillation in the Tropical Atmosphere
Huang Ronghui and Cui Xuefeng 337
- Extraseasonal Prediction of Summer Rainfall Anomaly over China with
Improved IAP PSSCA
Lin Zhaohui, Li Xu, Zhou Guangqing, Zhao Yan and Zeng Qingcun..... 351
- Temporal Structure of the Western Pacific Warm Pool SST and Its Comparison
with Nino 3 SST
Ren Baohua, Huang Ronghui and Huang Gang 367
- Numerical Simulations on the Relationship between Indian Summer Monsoon
and El Nino
Mu Mingquan and Li Chongyin..... 377
- Raindrop Category Numerical Simulations of Microphysical Processes of
Precipitation Formation in Stratiform Clouds
Guo Xueliang, Huang Meiyuan, Xu Huaying and Zhou Ling 387

Temporal Structure of the Western Pacific Warm Pool SST and Its Comparison with Nino 3 SST*

Ren Baohua(任保华)

(Department of Earth and Space Science, University of Science and Technology of China, Hefei 230026)

Huang Ronghui(黄荣辉) and Huang Gang(黄刚)

(Institute of Atmospheric Physics, Chinese Academy of Sciences, Beijing 100080)

Manuscript received October 16, 1999.

It is well known that the western Pacific warm pool (WWP), having the highest SST of the global oceans, plays an essential role in the global circulation and Asian monsoon. This work aims at disclosing temporal structure of the western Pacific warm pool SST by wavelet transform technique and comparing them with that in Nino 3. The data used is the GISST2.2 monthly dataset compiled by U.K. meteorological office from January 1903 to December 1994, which is $1^\circ \times 1^\circ$. The Morlet complex wavelet function was chosen for the wavelet analysis. The results show that the SST in WWP and Nino 3 have multi-scale variations with prominent period appearing in the interannual time scale (IAV: 2 yr-8 yr) which exceed 95% confidence testing. The peak is about 6 yr in WWP and 3 yr in Nino 3. There is a gradually IAV shift from 4-8 yr to about 2-4 yr after the mid-1960s in WWP and an abrupt IAV shift to even lower period in Nino 3 from mid-1960s to 1990s which might imply frequent occurrence of El Nino (La Nina) events. Moreover, the wavelet transform reveals that the multi-decadal signals are more important in modulating the variability of SST in WWP than in Nino 3 though they were not examined by 95% confidence testing, which might suggest further investigation be needed by using some longer data records.

Key words: SST; El Nino; warm pool.

1. INTRODUCTION

It was known that the tropical Western Pacific has the highest SST in the whole global oceans, where might exist stronger air-sea interactions. Many studies showed that the warm pool is a critical component of the earth's climate (Fasullo and Webster, 1998), the thermal states in the warm pool and the convective activities there may play an important role in the interannual variability of the East Asian summer monsoon (Nitta, 1987; Huang and Li, 1987;

* This paper was supported by National Key Programme for Developing Basic Sciences (G1998040900- Part 1) and Key Research Programme of Chinese Academy of Sciences "KZ951-A1-203".

Huang and Lu, 1989; Kurihara, 1989; Ren and Huang, 1999). Therefore, a better understanding of the characteristics of the western warm pool is of great significance to the study of the global circulation, especially to the realization and prediction of the East Asian summer monsoon variability. The spatial distributions of the warm pool have been extensively documented and delineated by the 28°C isotherm. But the temporal structure of the warm pool is, up to date, poorly concerned, which therefore motivated the author attempting to do something upon this topic.

The goal of this paper will be concentrated on the delineation of the temporal features in the western warm pool SST and comparison with the variations of Nino 3 SST by means of wavelet transform. The wavelet analysis is an effective tool in analyzing localized variations of power to a time series, which has been widely used in geophysics, such as ENSO signals (Gu and Philander, 1995; Wang and Wang, 1996), the global SST signals (Lau and Weng, 1998), the dispersion of ocean waves (Meyers et al., 1993), the tropical convection (Weng and Lau, 1994), the turbulent flows (Farge, 1992), the multiple time scale of North China water resources (Yang and Song, 1999). But the above mentioned studies have concluded their analysis with wavelet merely in a qualitative way, lack of quantitative results. More recently, Torrence and Compo discussed the wavelet transform in detail and provided an easy-to-use wavelet analysis toolkit with statistical significance testing, thus putting the wavelet analysis in a relatively quantitative way (Torrence and Compo, 1998). We will utilize this method to detect the multi-scale feature of the western warm pool SST and compare them with the Nino 3 SST. The organization of this paper is as follows: Section 2 is the description of data and method; followed by the results analysis and discussion in Section 3, and the conclusion will be given in Section 4.

2. DATA AND METHODOLOGY

The dataset used in the paper is the U.K. Meteorological Office GISST2.2 monthly SST data which ranges from January 1903 to December 1994 with a spatial resolution $1^\circ \times 1^\circ$ (latitude by longitude) and covers the entire global ocean. We have made monthly SST data to seasonal ones firstly and then constructed 1903–1994 seasonal SSTA by subtracting each season's climatological mean. Two time series were then defined as the area SSTA mean (130–160°E; 5°S–5°N) for the western warm pool (hereafter as WWP) and the area SSTA mean (150–90°W; 5°S–5°N) for Nino 3, respectively. The linear trend had been removed from these two time series before they were analyzed by using wavelet transform.

The wavelet transform is a powerful tool in decomposing multiple timescale variabilities within a time series that it unfolds the entire spectrum of variability in one single analysis, displacing both phase and amplitude information simultaneously. There are many wavelet bases including orthogonal and nonorthogonal, real and complex. A complex Morlet wavelet base was preferred in this paper, which has the form of a plane wave modulated by a Gaussian. The reasons why we chose Morlet wavelet transform are based on: (1) It is commonly used in the realization of geophysical signals; (2) It is nonorthogonal that enables one to make so-called continuous wavelet transform (Farge, 1992); (3) It can return information about both amplitude and phase and is suitable to capture oscillatory behavior; (4) It holds good locality both in frequency and in time domains. To quantify the results, the Morlet wavelet power spectrum significance testing was applied in the paper by use of the method proposed by Torrence and Compo (1998). For more details, the readers may refer to Torrence and Compo (1998), Weng and Lau (1994), Lau and Weng (1998) and many others.

3. RESULTS ANALYSIS

3.1 Wavelet Power Spectrum

The wavelet power spectrum is shown in Figure 1. From Figure 1, one could see clearly the multiple timescale variability of WWP and Nino 3, ranging from interannual to decadal and multi-decadal. In the WWP, Morlet wavelet transform depicts a prominent 2–8 year interannual variability (IAV) with pronounced signal centered around 6 year. This IAV shows much nonstationary variability which was strongest from the mid-1930s to around the 1970s and was relatively strong before 1910s while it had lower variance between the late 1910s and

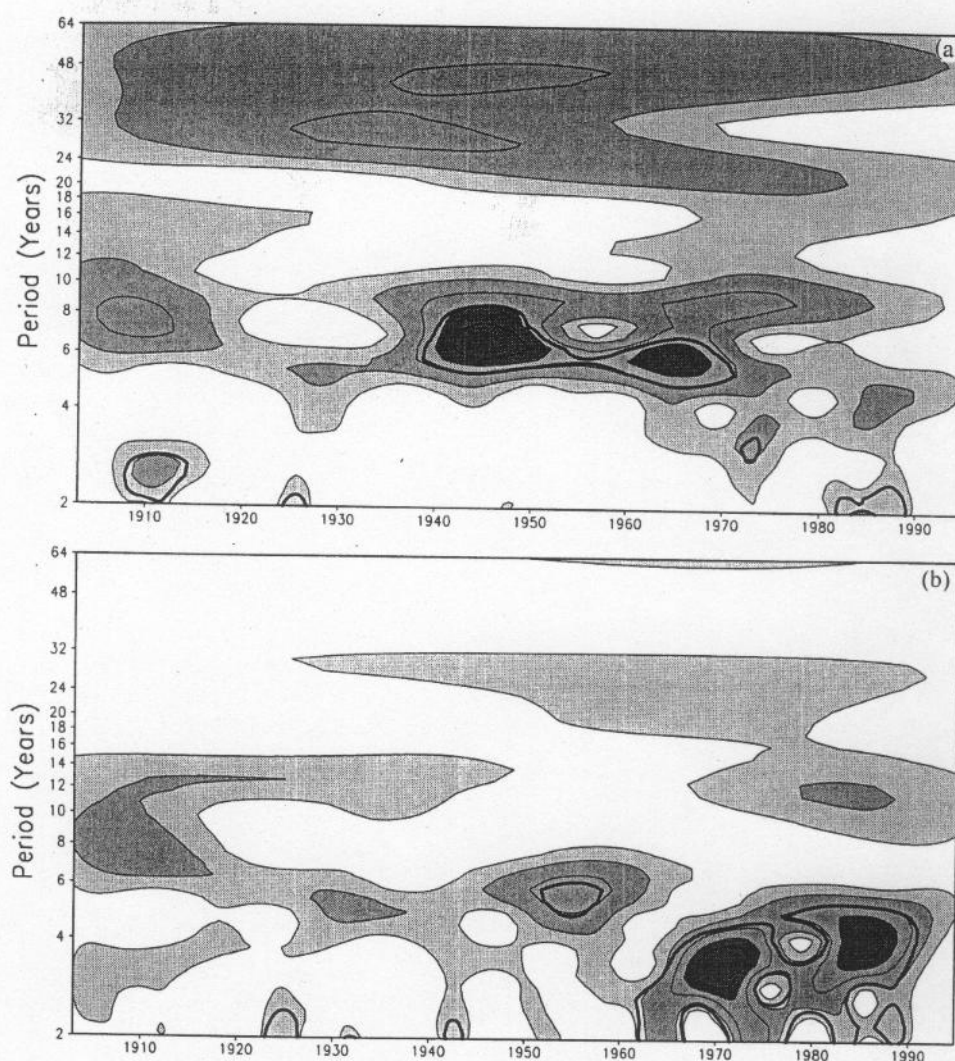


FIGURE 1. Morlet wavelet power spectrum for (a) WWP and (b) Nino 3. Shaded area denotes Values greater than 2 and intervals is 5, the thick-solid line is the 95% confidence line.

the mid-1930s. Also seen was a slight shift from 5–8 yr oscillation to 3–6 yr oscillation between the 1920s and the 1930s which might be viewed more clearly from its wavelet transform coefficients drawn in Figure 2a. Furthermore, both wavelet power spectrum (Fig.1a) and wavelet transform coefficients (Fig.2a) disclosed an IAV shift from about 5–8 yr oscillatory to lower period around 2–6 yr after 1965. Besides there existed decadal, bi-decadal to quadri-decadal variability in WWP as seen from Fig.1a and Fig.2a. But the 10–20 yr variance showed very weak indicative of dearth of 10–20 yr interdecadal oscillations. Another notable feature was that the decadal (10 yr) signal seems merged with IAV signal and could not be separated from IAV variability.

For Nino 3 SSTA, the Morlet wavelet transform also decomposed interannual, decadal to multidecadal signals as shown in Fig.1b and Fig.2b. The interannual (IAV) signal experienced large temporal variations, which was mainly concentrated in a 4–6 yr band roughly from the 1920s to the mid-1960s while there was a similar but rather abrupt shift from 4–6 yr

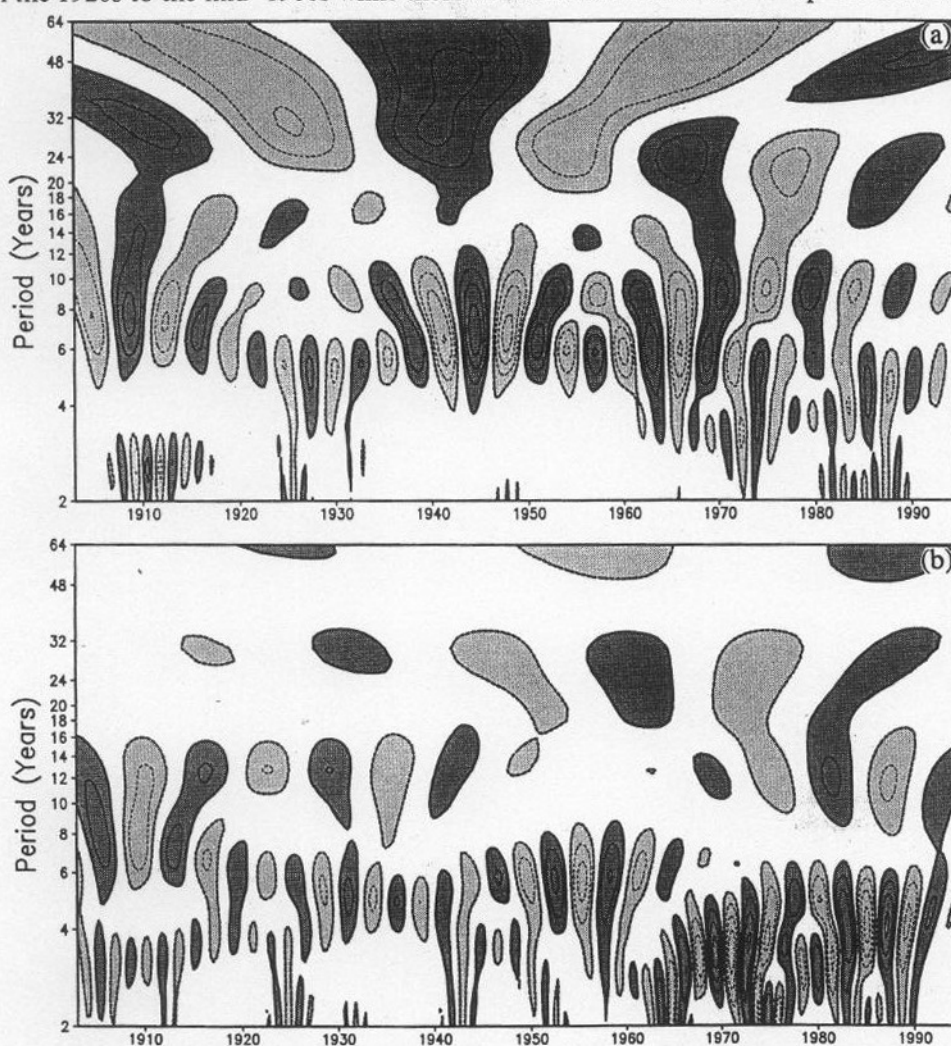


FIGURE 2. Morlet wavelet transform coefficients for (a) WWP and (b) Nino 3, heavy shaded area denotes positive coefficients and light shaded area for negative coefficients.

to 2–4 yr band compared with the IAV in WWP. As with longer period oscillations, the Nino 3 seems less robust in decadal to multidecadal signals with merely a quasi-decadal (10 yr) and a 20–30 yr interdecadal variances could be detected but weaker than IAV variance. Moreover, these two signals showed, to some extent, an out-of-phase temporal variation during the 1940s to the 1970s judged from Fig.1b and Fig.2b. To quantify the results, the wavelet power spectrum significance testing was applied. The method and procedure was adopted from Torrence (Torrence and Compo, 1998). The rough solid line in Fig.1 represents the 95% confidence level, which means the power enclosed by this line was detected significantly at 5% level. Based on this criterion, one could see from Fig.1 that in WWP, from the 1940s to the early 1970s, an IAV signal with 5–8 yr oscillations was strong and therefore could be a true feature. Meanwhile a 2–3 yr IAV signal around the 1910s and a quasi-2 yr signal in the mid-1920s were also noted and tested. It is interesting to find that a 3–4 yr oscillation in the early 1970s and a quasi-2 yr signal from the 1980s to the 1990s were examined against 95% confidence level, which implied that from the mid-1960s, an IAV shift from longer period to shorter period was a true feature significantly at 5% level. In Nino 3, similarly only IAV signals could be viewed as a true character at 5% significance level. The significant IAV signals also varied over time domain. Worthy of importance to note was the 95% confidence line (solid line in Fig.1b) enclosed 2–5 yr power from the mid-1960s to the 1990s indicating the significant variability during this period of time. In other word, an abrupt shift of IAV in the mid-1960s was detected to be a true climate signal not a background noise.

From above analyses, it is argued that the IAV (2–8 yr) variability was a true and main feature in both WWP and Nino 3 that could be disclosed at 95% confidence level. However no significant decadal to multi-decadal variability can be detected from the point of significance testing. On the other hand, as Figure 1 showed, the DIV (8–64 yr) power in WWP seems more pronounced than that in Nino 3, which might give a hint that besides IAV the DIV variability maybe more important in WWP than in Nino 3, in modulating the SST variability. This will be examined later.

3.2 Global Wavelet Power Spectrum

The wavelet transform translates a one-dimensional time series into a two-dimensional time–frequency domain. Thus one could average wavelet power either over time or over frequency to construct a time-averaged wavelet power spectrum or scale-averaged wavelet power spectrum, respectively. When applying time averaging over all time domains, one gives a so-called global wavelet spectrum which could provide a useful measure of the background spectrum against which peaks in the local wavelet spectrum could be tested.

The global wavelet power spectrum is shown in Fig.3 for WWP (upper panel) and for Nino 3 (lower panel). The solid line in the figure indicates the global wavelet spectrum and the dashed line is the 95% confidence level for the global wavelet spectrum, while the shaded area means the wavelet power exceeding 95% confidence level. Figure 3 clearly displays that a 5–7 yr signal peaked at 6 yr in WWP is found above 95% confidence level, implying a true feature in WWP SST, and a 2–5 yr period oscillation with a peak at 3 yr is seen to be tested by 95% confidence testing in Nino 3. Besides, the global wavelet spectrum in WWP (upper in Fig.3) depicts other two peaks comparable to 6 yr peak in around 9 yr and 40 yr, which could be respectively named as decadal (10 yr) and quadridecadal (40 yr) signals though they were not passed 95% confidence testing. However in Nino 3, two signals 10–15 yr and 20–30 yr appeared but weakened and failed to be tested at 95% confidence level.

The global wavelet power spectrum reveals that the detected signals at 95% confidence level concentrated within IAV band either in WWP or in Nino 3. Next we will explore IAV signal variability over time by scale averaging over 2–8 yr.

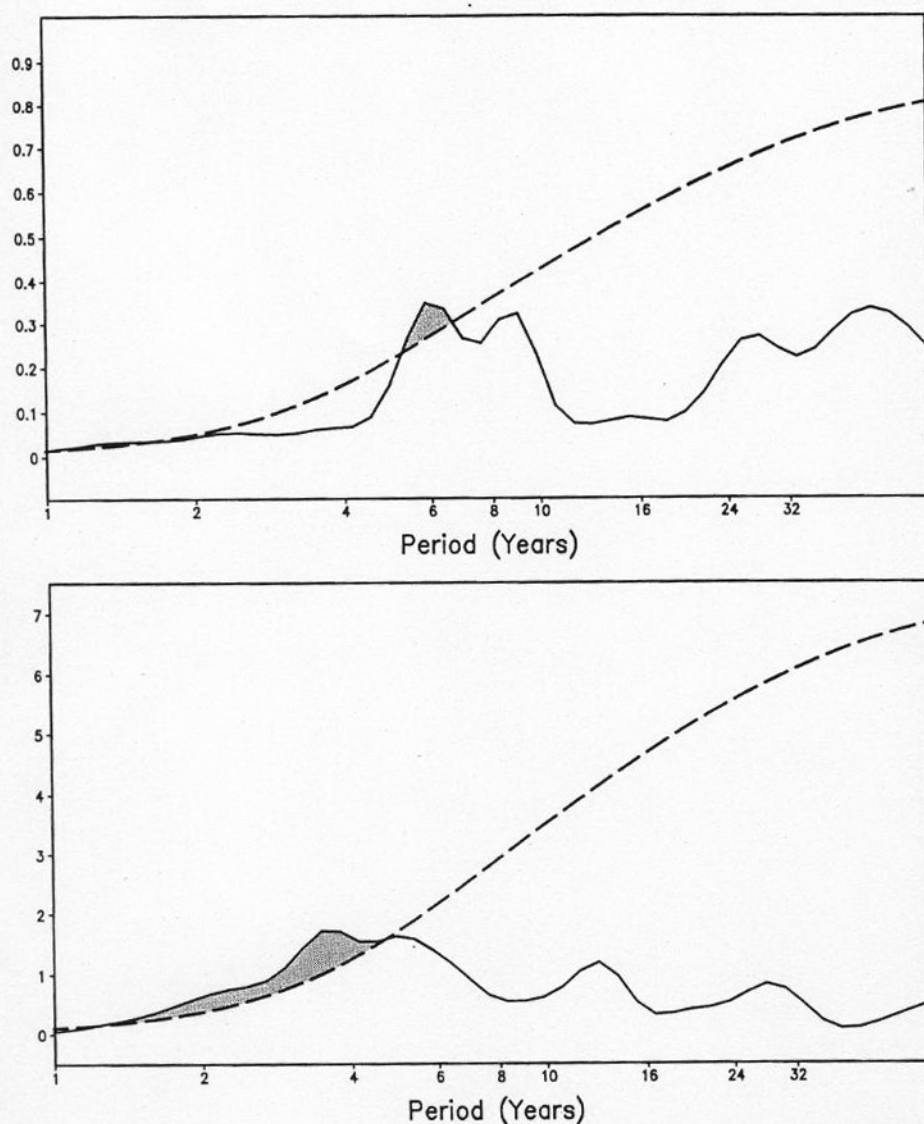


FIGURE 3. Global wavelet power spectrum by using Morlet for WWP (upper panel) and Nino 3 (lower panel). Dashed line indicates 95% confidence level, solid line is the power spectrum. Shaded means that the period passed 95% confidence test.

3.3 IAV Temporal Variations

By scale-averaging wavelet power spectrum over 2–8 yr, we plotted the IAV power spectrum in Fig.4. The solid line denotes IAV power spectrum over time and the dashed represents the 95% confidence level for scale-averaged wavelet spectrum, while the shaded area implies the power exceeding the 95% confidence level. It could be easy to see that the IAV in WWP (upper panel) fluctuates over time and is found to be significant during the mid-1960s. Moreover this IAV variability seems modulated by multidecadal variability as disclosed from the figure. The lower panel in Fig.4 shows a striking feature that from the mid-1960s to the 1990s the IAV signal in Nino 3 was very pronounced to exceed the 95% confidence level.

Nevertheless the IAV in Nino 3 seems less modulated by multidecadal variabilities, which is slightly different from Torrence and Compo (1998) in that they also detected a IAV signal between the late 1910s to the 1920s significant at 95% confidence level but we could not reveal such feature in Figure 4 (lower panel). This difference might be due to the different dataset used for they used a longer SST dataset from 1871 to 1997.

As many studies argued that the wavelet transform is essentially a bandpass filter of uniform shape and varying location and width. Therefore one could construct a wavelet-filtered time series at ease. For details, interested readers may refer to Torrence and Compo (1998). To investigate the relationship between SSTA and its IAV (2–8 yr) component and DIV (8–64 yr) component, we have reconstructed IAV and DIV SSTA time series as shown in Fig.5 and Fig.6, respectively. The simultaneous coefficients between SSTA and IAV SSTA

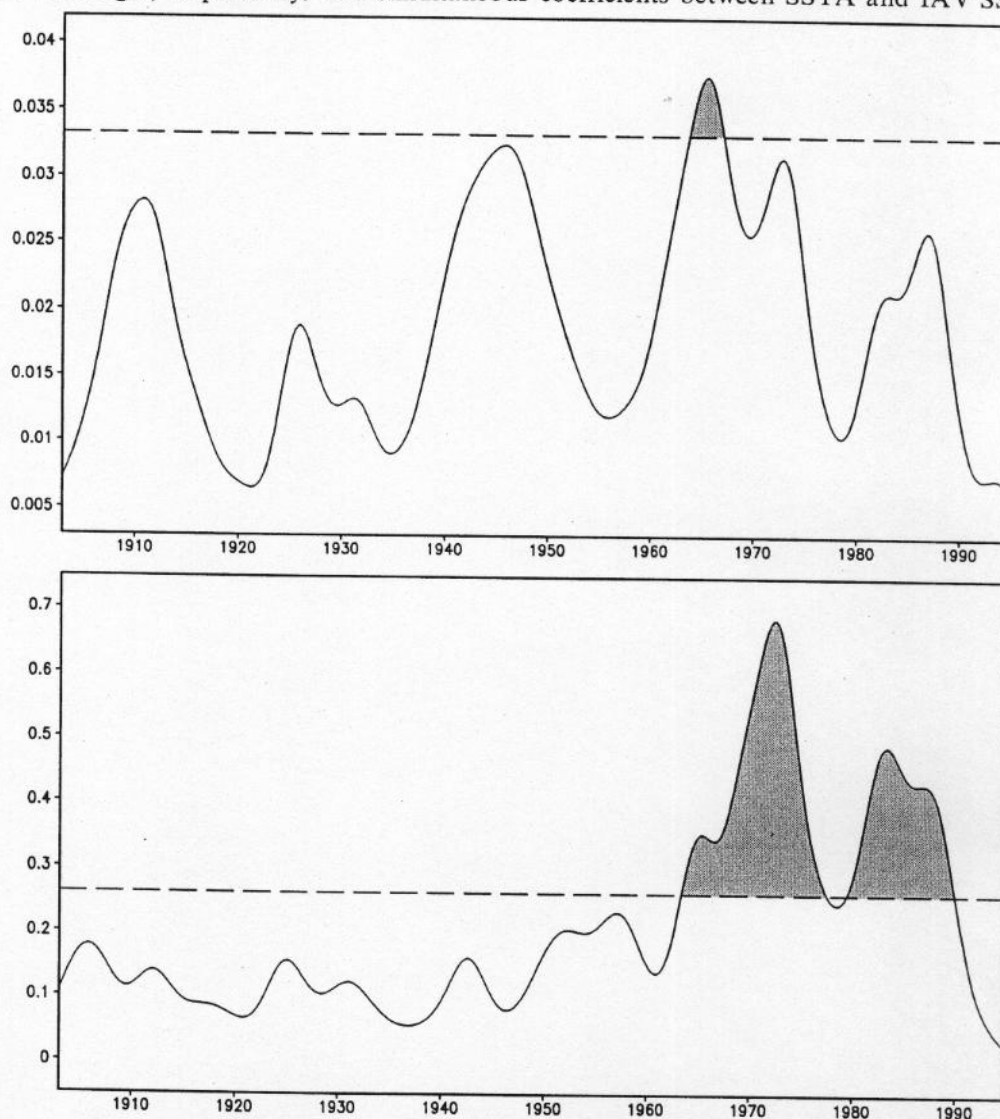


FIGURE 4. IAV (2–8 year) scale-averaged power spectrum for WWP (upper panel) and Nino 3 (lower panel), the dashed line indicates 95% confidence level and the shaded area means the variance exceeding 95% confidence test.

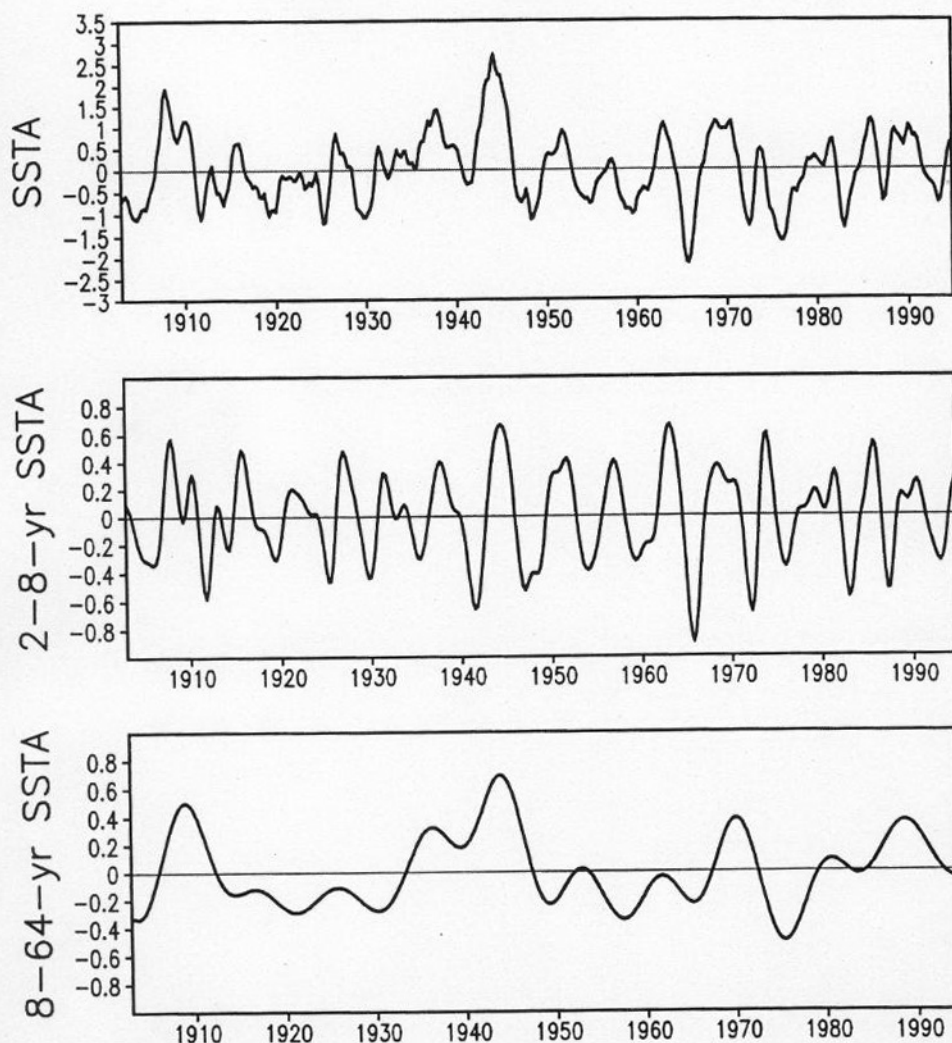


FIGURE 5. Seasonal SSTA (upper), its reconstructed 2–8 yr (IAV) component (middle) and 8–64 yr (DIV) component in WWP. The simultaneous coefficient between SSTA and IAV is 0.75, and 0.58 with DIV.

are 0.75 and 0.85 in WWP and in Nino 3, respectively, while the simultaneous coefficients between SSTA and DIV SSTA are 0.58 and 0.38 in WWP and in Nino 3, respectively. These results coincide with our former discussion that the IAV dominates the variability of SSTA in both WWP and Nino 3, whereas the DIV signal is more important in WWP than in Nino 3 in modulating the variability of SSTA.

4. SUMMARY AND CONCLUSION

Wavelet transform reveals that there exist interannual (IAV) and Interdecadal (DIV) variability in WWP and Nino 3 with dominant SSTA variability concentrated in IAV band. In WWP, the IAV is within 4–8 yr centered at about 6 yr with large fluctuations over time. Between the 1940s and the 1970s, the IAV in WWP was significantly strong, while it showed weakened variance in between the 1920s and the 1940s. Moreover, there is a gradually IAV

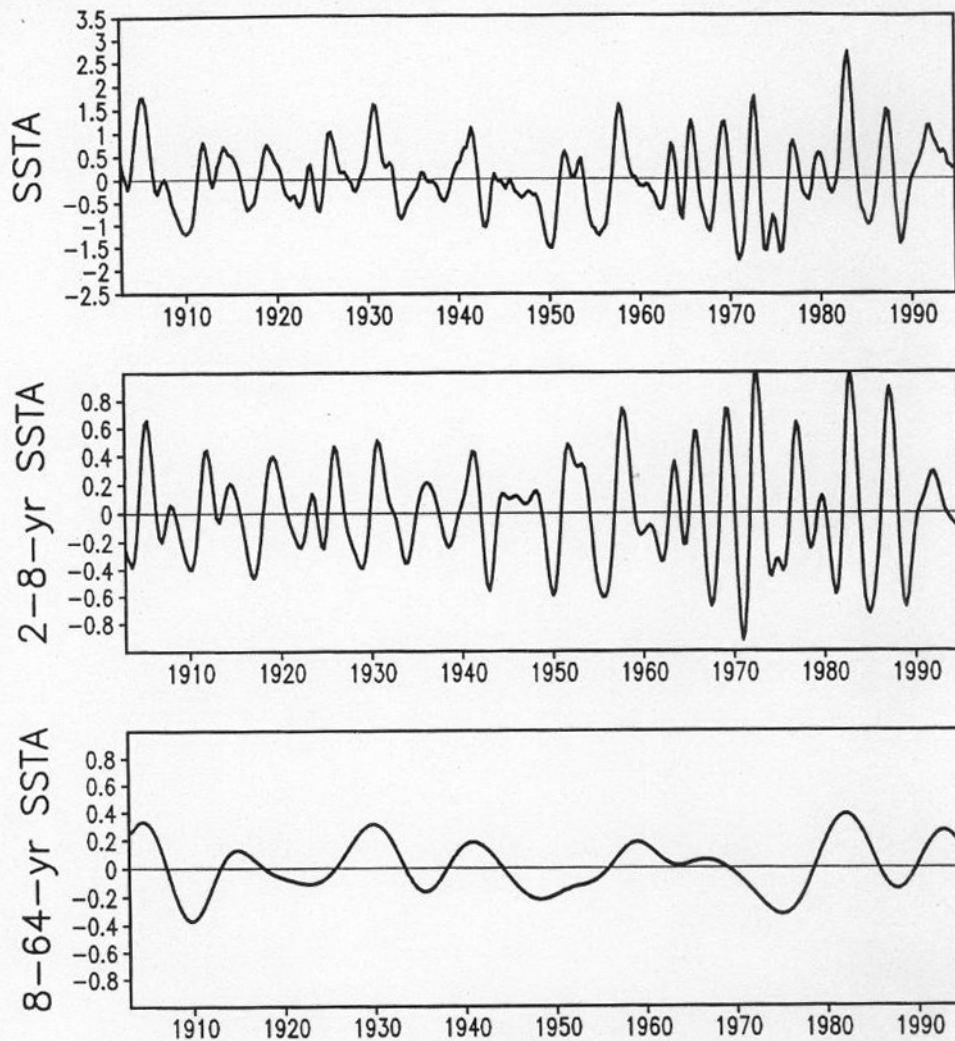


FIGURE 6. Seasonal SSTA (upper), 2–8 yr (IAV) component (middle) and 8–64 yr (DIV) component (bottom) in Nino 3. The simultaneous coefficient between SSTA and IAV is 0.85 and 0.38 with DIV.

shift from 4–8 yr to about 2–4 yr after the mid-1960s. Similarly in Nino 3, the variability of SSTA was found largely in IAV but with a lower 2–6 yr timescale. An abrupt IAV shift to even lower period was also detected in the mid-1960s, which might imply frequent occurrence of El Nino (La Nina) events. As for interdecadal signals, differences exist between WWP and Nino 3 that a decadal, tridecadal and quadridecadal signals was found in WWP though they did not pass 95% confidence testing. In Nino 3, the decadal and bidecadal to tridecadal signals are relatively weaker compared to WWP. No quadridecadal signal was found in Nino 3 as that in WWP. This will be worthy of investigating further.

IAV power spectrum shows that in Nino 3, from about the mid-1960s to the 1990s, the power was pronounced very large at 95% confidence level indicating the intensification of ENSO-like signals. Before the mid-1960s, the IAV power was very low. In WWP, only in the mid-1960s that the IAV showed variability significantly at 95% confidence level. The IAV in WWP was modulated by interdecadal variability ranging from 10 yr to even 40 yr. Neverthe-

less in the Nino 3, the IAV seems less influenced by interdecadal variability. The reconstructed IAV-SSTA and DIV-SSTA show that in Nino 3, the variability of SSTA seems largely dependant on IAV variability, while in WWP the SSTA might be influenced not only by IAV but also, to some extent, by DIV variances.

The decadal to multidecadal signals did not pass the 95% confidence testing though they seem more crucial in modulating the variability of SSTA in WWP than in Nino 3. This might be partially due to the limitation of data records used in the paper. Therefore, further study should be conducted by employing new dataset with longer data records.

REFERENCES

- Farge, M., 1992: Wavelet trnsforms and their applications to turbulence, *Annu. Rev. Fluid Mech.*, **24**, 395-457.
- Fasullo, J., Webster, P. J., 1999: Warm Pool SST variability in relation to the surface energy balance, *J. Climate*, **12**, 1292-1305.
- Gu, D. and S. G. H. Philander, 1995: Secular changes of annual and interannual variability in the Tropics during the past century, *J. Climate*, **8**, 864-876.
- Huang Ronghui and Li Weijing, 1987: Influence of the heat source anomaly over the tropical western Pacific on the subtropical high over East Asia, *Proceedings of the International Conference on the General Circulation of East Asia*, Chengdu, April 10-15, 1987, 40-51.
- Huang Ronghui and Lu Li, 1989: Numerical simulation of the relationship between the anomaly of the subtropical high over East Asia and the convective activities in the western tropical Pacific, *Adv. Atmos. Sci.*, **6**, 202-214.
- Kurihara, K., 1989: A climatological study on the relationship between the Japanese summer weather and the subtropical high in the western northern Pacific, *Geophys. Mag.*, **43**, 45-104.
- Lau, K. M. and H. Weng, 1998: Interannual, decadal-interdecadal, and global warming signals in sea surface temperature during 1955-97, *J. Climate*, **12**, 1257-1267.
- Meyers, S. D., B. G. Kelly and J. J. O'Brien, 1993: An introduction to wavelet analysis in oceanography and meteorology: with application to the dispersion of Yanai waves, *Mon. Wea. Rev.*, **121**, 2858-2866.
- Nitta, Ts., 1987: Convective activities in the tropical western Pacific and their impact on the Northern Hemisphere summer circulation, *J. Meteor. Soc. Japan*, **64**, 373-390.
- Ren Baohua and Huang Ronghui, 1999: Interannual variability of the convective activities associated with the East Asian summer monsoon obtained from TBB variability, *Adv. Atmos. Sci.*, **16**, 77-90.
- Torrence, C. and G. P. Compo, 1998: A practical guide to wavelet analysis, *Bull. Amer. Meteor. Soc.*, **79**, 61-78.
- Wang, B. and Y. Wang, 1996: Temporal structure of the Southern Oscillation as revealed by waveform and wavelet analysis, *J. Climate*, **9**, 1586-1598.
- Weng, H. and K.-M. Lau, 1994: Wavelets, period doubling, and time-frequency localization with application to organization of convection over the tropical western Pacific, *J. Atmos. Sci.*, **51**, 2523-2541.
- Yang, H., and Song Zhengsan, 1999: Multiple timescale analysis over Northern China water resources, *Plateau Meteor.*, **18**, 496-508. (in Chinese)